Correlations of the First Normal Stress Difference with Shear Stress and of the Storage Modulus with Loss Modulus for Homopolymers

CHANG DAE HAN, *Department of Chemical Engineering, Polytechnic Institute of New York, Brooklyn, New York 11201* and MYUNG S. JHON, *Department of Chemical Engineering, Carnegie-Mellon University, Pittsburgh, Pennsylvania 15213*

Synopsis

The effects of temperature, molecular weight and its distribution, side chain branching, and the structure of polymers on the elastic behavior of bulk homopolymers were investigated, by using logarithmic plots of first normal stress difference (N_1) against shear stress (σ_{12}) and logarithmic plots of storage modulus (G') against loss modulus (G''). For the investigation, we have used data from the literature as well as our recent experimental results, covering a very wide range of temperature and shear stress or loss modulus. It has been found that such plots are very weakly sensitive to (or virtually independent of) temperature and to the molecular weight of high molecular weight polymers, but strongly dependent upon the molecular weight distribution and the degree of side chain branching. A theoretical interpretation of the observed correlations is presented, using molecular theories.

INTRODUCTION

During the past three decades numerous investigators have measured the viscoelastic properties of polymeric liquids, using a variety of experimental techniques. Recent monographs[1-3] describe both the theoretical backgrounds and the experimental techniques of the rheological measurements. Among the techniques, the one measuring steady and/or oscillatory shear flow properties has been used most extensively. This is primarily due to the fact that the kinematics associated with a shearing flow field is rather simple, and consequently an interpretation of experimental data is straightforward.

In steady shear flow, the variables that one usually measures are the shear rate ($\dot{\gamma}$), the shear stress (σ_{12}) [or the shear viscosity (η)], the first normal stress difference (N_1), and sometimes the second normal stress difference (N_2). In oscillatory shear flow, one measures the frequency (ω), the storage modulus (G'), and the loss modulus (G'') [or the dynamic viscosity (η')]. The theoretical background of the methods for calculating various quantities of rheological interest are well documented in the literature.[1-3]

Let us consider a cone-and-plate rheometer or concentric cylinder rheometer. In interpreting rheological data obtained from an instrument having this flow geometry, one usually plots N_1 and σ_{12} (or η) against $\dot{\gamma}$, and G' and G'' (or η') against ω and discusses the effects of, for instance, molecular weight and structure of polymers on their rheological properties (namely, σ_{12}, N_1, G', and G''). In the past, some attempts[4-6] were made to relate η

Journal of Applied Polymer Science, Vol. 32, 3809–3840 (1986)
 CCC 0021-8995/86/033809-32$04.00

to η', and N_1 to G' of polymeric liquids by shifting the scale of $\dot{\gamma}$. Also, a phenomenological theory[7] was developed to relate steady shear flow measurements to oscillatory shear flow measurements at low values of $\dot{\gamma}$ and ω.

Starting about a decade ago, Han and co-workers[8-24] have shown that the use of logarithmic plots of N_1 vs. σ_{12} (instead of N_1 vs. $\dot{\gamma}$) gives rise to correlations which become virtually independent of temperature. They have shown that such plots may be useful for investigating the effects on the elastic behavior of polymers of their molecular weight distribution, their degree of long-chain branching, and their structure.[13,15,16,19-21] Furthermore, they have used such plots to interpret the rheological behavior of two-phase polymer blends[9,11-13,18,22-24] and interfacial instability occurring in stratified two-phase flow (i.e., coextrusion).[10,13,14,17,18] More recently, White and co-worker[25-30] also began to use logarithmic plots of N_1 vs. σ_{12} to interpret their rheological measurements of homopolymers and polymer blends.

Oscillatory shear flow data have long been used for the rheological investigation of polymeric liquids. During the past decades, substantial amounts of oscillatory shear flow data have become available in the literature[31-40] for bulk polymers (namely, thermoplastic melts and elastomers). All this literature data was presented in terms of G' and/or G'' vs. ω, often using the reduced variable ωa_T, in which a_T is a shift factor that varies with temperature.[3]

Recently, Han and co-workers[19,22,24] have shown that the use of logarithmic plots of G' vs. G'' (instead of G' vs. ω) for a variety of polymer melts gives rise to correlations that are virtually independent of temperature and that such plots are very useful for interpreting the rheological behavior of compatible and incompatible polymer blends, in a manner exactly the same as in the use of logarithmic plots of N_1 vs. σ_{12}. Apparently inspired by the Cole–Cole plot,* Harrell and Nakajima[45] also used logarithmic plots of G' vs. G'' to interpret the effects of the degree of long-chain branching of ethylene–propylene copolymers on their rheological behavior.

In this paper we will present the published data on oscillatory shear flow for a variety of homopolymers, together with our more recent data, using plots of log G' vs. log G'' and then compare, where possible, the correlations of log G' vs. log G'' with the correlations of log N_1 vs. log σ_{12}, with emphasis on the effects of temperature, molecular weight, molecular weight distribution, and the degree of long-chain branching on the elastic behavior of bulk polymers. Finally we will present a theoretical interpretation of log G'–log G'' (and log N_1–log σ_{12}) correlations, using molecular theories.

EXPERIMENTAL CORRELATIONS

We will first present experimental correlations between log G' and log G'', using the literature data of oscillatory shear flow for bulk polymers that have narrow molecular weight distribution and then, present correlations between log N_1 and log σ_{12}, and between log G' and log G'', using

* Cole and Cole[41] used the ordinary coordinate system to plot the real part (ϵ') of the complex dielectric constant on the abscissa against imaginary part (ϵ'') on the ordinate, for a number of polar materials at various temperatures. Other investigators[42-44] also used the Cole–Cole plot to interpret the dynamic mechanical properties of polymeric materials in the solid state.

our own recent data of steady and oscillatory shear flows for commercial polymers that have broad molecular weight distribution. When presenting the literature data, we will use the symbols and notations that appeared in the original papers.

It should be mentioned that the rheological data that will be presented below were obtained with either a cone-and-plate rheometer or a concentric cylinder rheometer. Note that the use of the rotational instrument for polymeric melts is limited to low shear rates. The range lies below 10 s^{-1} for most commercially available molten polymers, although the exact upper limit of operable shear rate may vary from material to material. In oscillatory shear flow, values of G' and G'' were measured as a function of ω, and in steady shear flow, values of N_1 and σ_{12} as a function of $\dot{\gamma}$. The basic principles and the mathematical formulas used in the analyses of the experimental data are well documented in the literature,[1-3] and therefore, in order to save space, we shall not repeat it here.

Linear Homopolymers with Narrow Molecualr Weight Distribution

Figure 1 gives plots of log G' and log G'' vs. log ω for linear polybutadiene (PB) at 24.5°C, as obtained by Rochefort et al.[38] and Table I gives data on the molecular characteristics of the polymer samples. Note that the molecular weight distribution (MWD) (i.e., $\overline{M}_w/\overline{M}_n$ ratio) of these materials is 1.05, in which $\overline{M}_w$ is the weight-average molecular weight and $\overline{M}_n$ is the number-average molecular weight. Figure 2 gives log G'–log G'' plots for the linear PB's, using the data displayed in Figure 1. It is seen in Figure 2 that the log G'–log G'' plot gives a correlation only slightly sensitive to the molecular weight of the polymer samples tested, in the region where log G' and log G'' follow a linear relationship. It is of interest to note in Figure 2 that, at a given value of G'', G' has dual values for the high molecular-weight PB samples (347L and 813L). This is due to the fact that, as may be seen in Figure 1, G'' goes through a maximum while G' approaches a constant value as the frequency (ω) is increased.

Figure 3 shows the effect of temperature when log G' and log G'' are plotted against log ω, for the linear polybutadiene PB–813L. The numerical data used in Figure 3 were supplied to us by Dr. W. W. Graessley at Exxon Research Engineering Co. Figure 4 gives log G'–log G'' plots for the PB-813L, with the same data used in Figure 3. It is seen that the temperature effect is virtually eliminated in the region where log G' and log G'' follow a linear relationship.

Figure 5 gives plots of log G' and log G'' vs. log ωa_T for anionic polystyrenes (PS) measured over a wide range of frequency and temperature by Onogi et al.[32] Note in Figure 5 that the data taken at various temperatures were reduced by using a shift factor a_T (i.e., by use of the time–temperature superposition principle). Table II gives data on the molecular characteristics of the PS samples. Figure 6 gives log G'–log G'' plots for the anionic PSs, using the data displayed in Figure 5. It is seen in Figure 6 that the log G'–log G'' plots become virtually independent of molecular weight of the polymer samples tested. Note in Table II that sample L18 has a molecular weight about 20 times as large as that of sample L14, and yet the $\overline{M}_w/\overline{M}_n$ ratio of the two samples is roughly the same, i.e., $\overline{M}_w/\overline{M}_n < 1.20$.

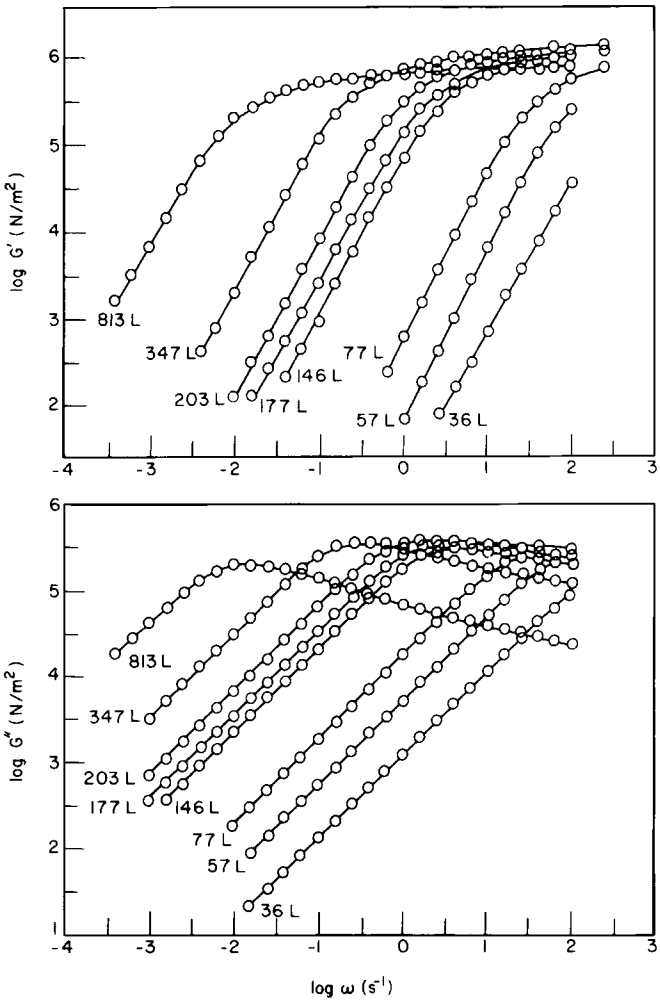

Fig. 1. log G' and log G'' vs. log ω for linear polybutadienes at 24.5°C.[38]

Effect of Molecular Weight Distribution

Figure 7 gives plots of log G' and log G'' vs. log ωa_T for anionic poly(methyl methacrylate) (PMMA) measured over a wide range of frequency and temperature by Masuda et al.,[34] and Table III gives data on the molecular characteristics of the PMMA samples. Figure 8 gives log G'–log G'' plots for the anionic PMMA samples, using the data displayed in Figure 7. Note that these plots exhibit a mild dependence on MWD (i.e., $\overline{M}_w/\overline{M}_n$ ratio) of the PMMA samples tested (see Table III). The effect of MWD on log G'–log G'' plots can clearly be illustrated from the following PS samples.

Figure 9 gives plots of log G' and log G'' vs. log ωa_T, and Table IV data on the molecular characteristics for anionic PSs measured over a wide range of frequency and temperature by Masuda et al.[33] Figure 10 gives log G'–log G'' plots for the anionic PSs, using the data displayed in Figure 9. It is seen in Figure 10 that sample PS7, having a broader MWD ($\overline{M}_w/\overline{M}_n$ = 1.84), has greater values of G' than sample L15, which has a narrower MWD ($\overline{M}_w/\overline{M}_n$ = 1.13).

TABLE I
Molecular Characteristics Data for Linear and Star-Branched Polybutadienes at 24.5°C 38

Sample	$(\overline{M}_w)_{LS} \times 10^{-3}$	$(\overline{M}_n)_{OS} \times 10^{-3}$	$(\overline{M}_w)_{GPC} \times 10^{-3}$	$\left(\frac{\overline{M}_w}{\overline{M}_n}\right)_{GPC}$	$[\eta]_{THF}$
Linear PB					
36L	—	—	35.8	1.05	0.591
57L	—	—	56.7	1.05	0.835
77L	73.3	71.4	77.4	1.05	1.05
146L	141	—	146	1.05	1.70
177L	174	—	177	1.05	1.96
203L	199	196	203	1.05	2.17
347L	365	295	347	1.05	3.25
813L	791	700	813	1.05	6.15
Four-Star PB					
42S4	24	25.5	42.3	1.08	0.401
88S4	84.5	80.3	87.5	1.09	0.935
173S4	—	—	173	1.14	1.30
217S4	259	164	217	1.24	1.51

LS = light scattering weight-average molecular weight; OS = membrane osmometer number-average molecular weight; GPC = gel permeation chromatography; and THF = tetrahydrofuran.

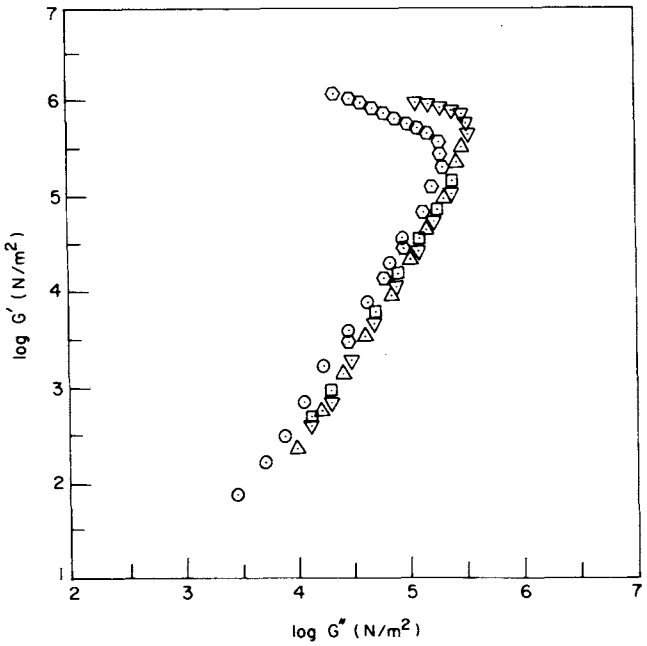

Fig. 2. log G' vs. log G'' for linear polybutadienes, which are the same materials as in Figure 1: (⊙) 36L; (△) 77L; (⊡) 146L; (▽) 347L; (⊙) 813L.

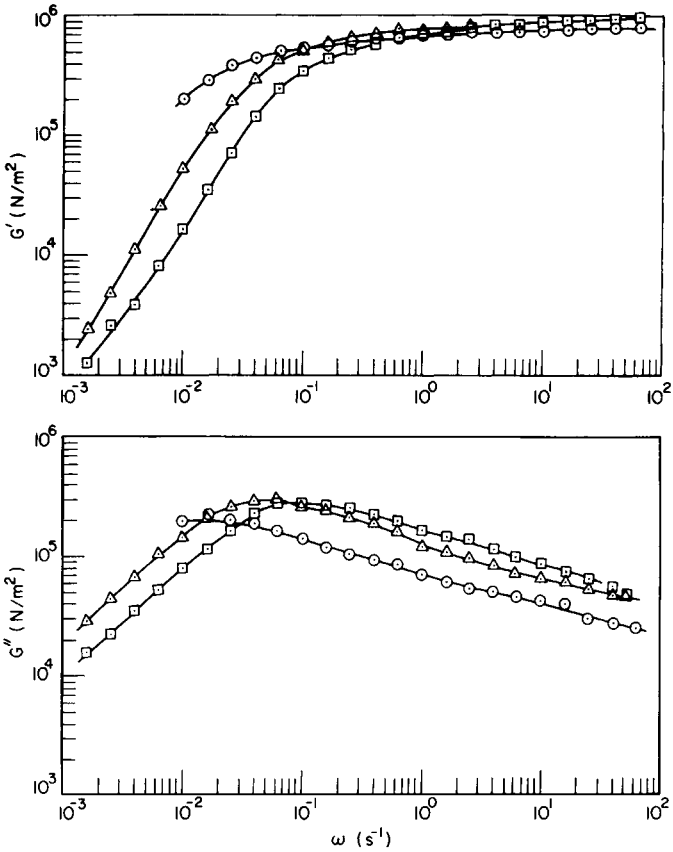

Fig. 3. log G' and log G'' vs. log ω for the linear polybutadiene PB-813L at three different temperature (°C): (⊙) 24.5; (△) 50; (⊡) 75.

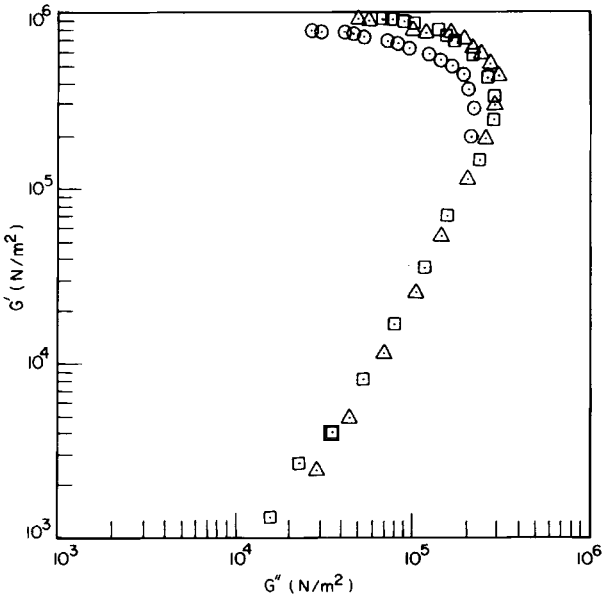

Fig. 4. log G' vs. log G'' for the linear polybutadiene PB-813L at three different temperatures. Symbols are the same as in Figure 3.

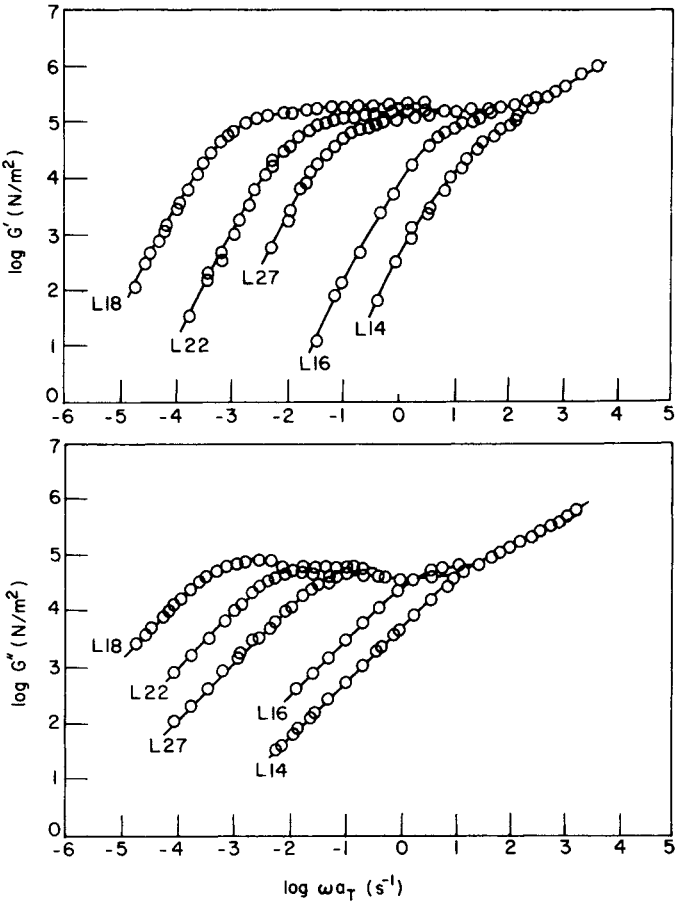

Fig. 5. log G' and log G'' vs. log ωa_T for polystyrenes. The reference temperature is 160°C.[32]

Effect of Side Chain Branching

Figure 11 gives plots of log G' and log G'' vs. log ωa_T, and Table I gives data on the molecular characteristics, for four-star branched polybutadienes measured over a wide range of frequency and temperature by Rochefort et al.[38] Figure 12 shows the effect of temperatue when log G' and log G'' are plotted against log ω for the branched polybutadiene PB-217S4, used in Figure 11. Figure 13 gives log G'–log G'' plots for the four-star branched PBs, using the data displayed in Figure 11. The numerical data used in Figures 12 and 13 were supplied to us by Dr. W. W. Graessley. It is important

TABLE II
Molecular Characteristics Data for Polystyrenes[32]

Sample code	$\overline{M}_n \times 10^{-3}$	$\overline{M}_w \times 10^{-3}$	$\overline{M}_w/\overline{M}_n$
L14	24.3	29	1.20
L16	52.3	59	1.13
L27	164	185	1.13
L22	288	318	1.10
L18	563	616	1.09

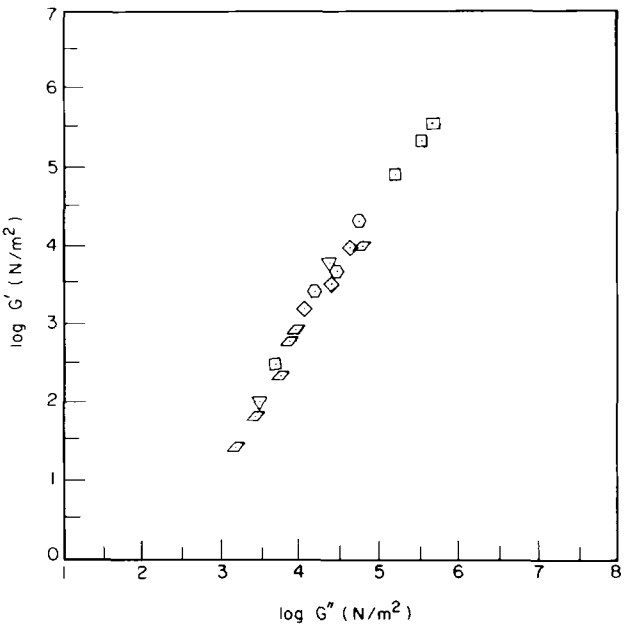

Fig. 6. log G' vs. log G'' for linear polystyrenes, which are the same materials as in Figure 5: (⊡) L14; (▽) L16; (◇) L27; (◈) L22; (⊙) L18.

to notice that the plots given in Figure 13 are virtually independent of temperature. It should be pointed out that such observation has been reported with commercial polymers by Han and co-workers.[19,22,24]

It is seen in Figure 13 that the value of G' become greater as the MWD is broadened. A close examination of Table I reveals that the MWD of the branched PBs is much more sensitive to an increase in molecular weight than that of the linear PBs. In other words, an introduction of star branching to linear PBs appears to have broadened their MWD. Moreover, a comparison of Figure 13 with Figure 2 reveals that the values of G' for the star-branched PBs are considerably greater than those for the linear PBs.

Figures 14 and 15 give log G'–log G'' plots for four-arm and six-arm star polystyrenes, respectively, measured over a wide range of frequency and temperature by Graessley and Roovers.[39] These plots are prepared with the numerical data received from Dr. J. Roovers at the National Research Council of Canada, and Table V gives data on the molecular characteristics of the star-branched PSs. It is clear from Figures 14 and 15 that G' increases with increase in weight-average molecular weight ($\overline{M}_w$). Judging from the molecular characteristics data for star-branched PBs given in Table I, we can surmise that the $\overline{M}_w/\overline{M}_n$ ratio for the star-branched PSs given in Table V also increases with $\overline{M}_w$, and therefore we can conclude that the observed increase in G' given in Figures 14 and 15 is attributable in part to the increase in the $\overline{M}_w/\overline{M}_n$ ratio, i.e., the broadening of the MWD.

Commercial Polymers

Figure 16 gives MWD curves for three different grades of commercial low-density polyethylene (LDPE), and Table VI gives data on the molecular characteristics of the LDPEs. Note in Table VI that the degree of long-

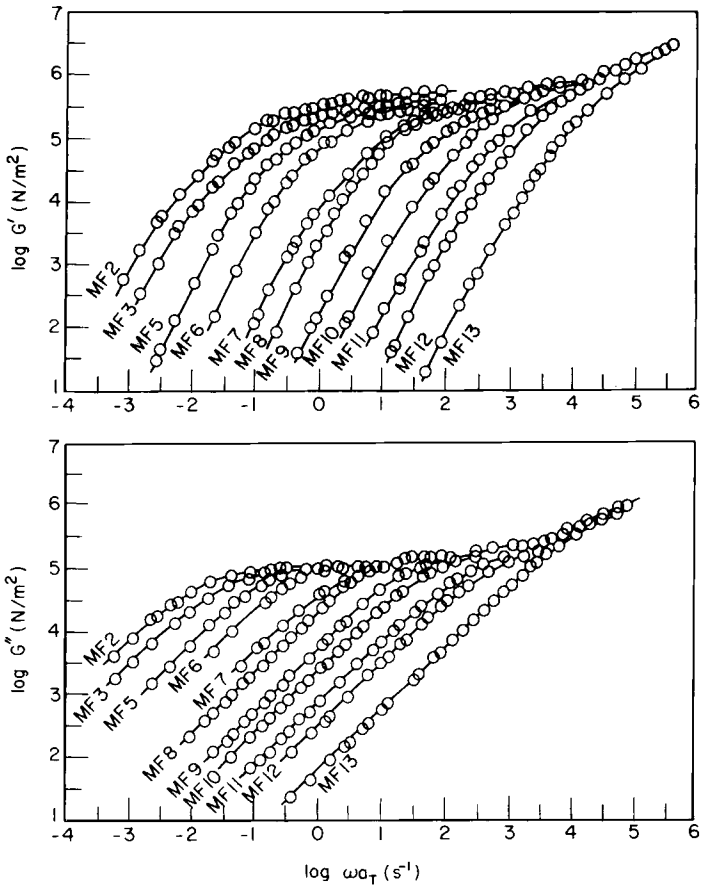

Fig. 7. log G' and log G'' vs. log ωa_T for poly(methyl methacrylate)s. The reference temperature is 220°C.[34]

chain branching (LCB) increases with increase in $\overline{M}_w/\overline{M}_n$ ratio. Figure 17 gives plots of log N_1 vs. log $\dot{\gamma}$, and log G' versus log ω, for LDPE-A at three temperatures, 180, 200, and 220°C. Similar plots are given in Figure 18 for LDPE-B and in Figure 19 for LDPE-C. It is seen, in Figures 17–19, that both N_1 and G' decrease as the temperature increases. However, log N_1 –

TABLE III
Molecular Characteristics Data for Poly(methyl Methacrylate)s[34]

Sample	$\overline{M}_w \times 10^{-3}$	$\overline{M}_n \times 10^{-3}$	$\overline{M}_w/\overline{M}_n$
MF2	342	224	1.63
MF3	270	118	1.44
MF5	197	146	1.35
MF6	158	139	1.14
MF7	116	98.0	1.18
MF8	96.3	71.8	1.34
MF9	63.9	52.8	1.21
MF10	45.2	37.1	1.22
MF11	35.1	25.3	1.39
MF12	28.4	18.0	1.58
MF13	11.4	9.1	1.35

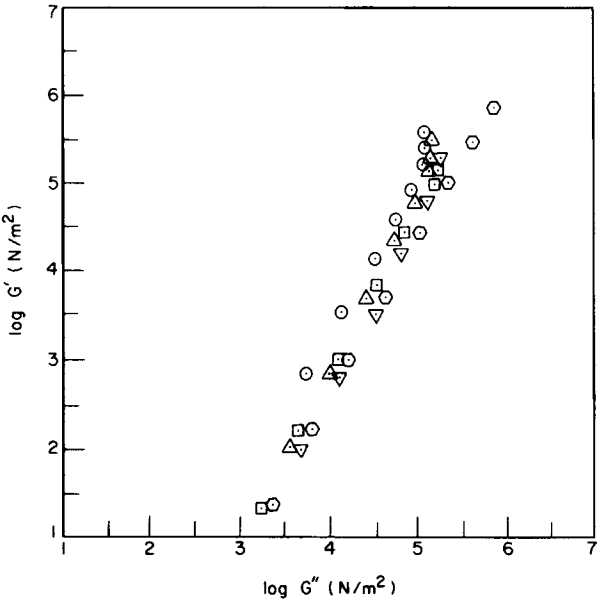

Fig. 8. log G' vs. log G'' for poly(methyl methacrylate)s, which are the same materials as in Figure 7: (⊙) MF2; (△) MF6; (⊡) MF9; (▽) MF12; (⊙) MF13.

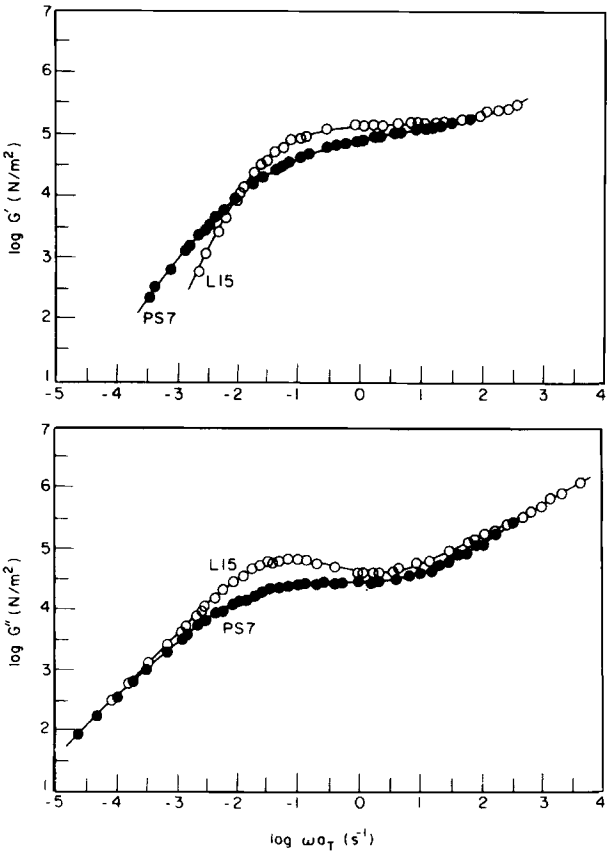

Fig. 9. log G' and log G'' vs. log ωa_T for polystyrenes. The reference temperature is 160°C.[33]

TABLE IV
Molecular Characteristics Data for Polystyrenes[33]

Sample	$\overline{M}_w \times 10^{-3}$	$\overline{M}_n \times 10^{-3}$	$\overline{M}_w/\overline{M}_n$
L15	229	203	1.13
PS7	313	170	1.84

log σ_{12} and log G'–log G'' plots, respectively, give rise to correlations that become virtually independent of temperature, as shown in Figures 20–22. Similar observations have been made by Han and co-workers.[10,12,14,15,17-23]

Figure 23 displays the effect of the degree of LCB on log N_1–log σ_{12} and log G'–log G'' plots. It is seen in Figure 23 that LDPE-A, with the highest degree of LCB of the three LDPEs, exhibits the largest values of N_1 and G'. This observation is consistent with the observation made on the star-branched PBs (see Fig. 13) and the star-branched PSs (see Figs. 14 and 15). It can be concluded therefore that the greater the degree of side-chain branching, the larger the values of N_1 in the log N_1–log σ_{12} plots and of G' in the log G'–log G'' plots.

THEORETICAL INTERPRETATION

We will now give a theoretical interpretation of the experimental correlations presented above. It is a well-accepted fact today that the first normal stress differnce N_1 in steady shear flow and the storage modulus G' in oscillatory shear flow may be considered as the amount of energy stored in a viscoelastic liquid. Also, the shear stress σ_{12} in steady shear

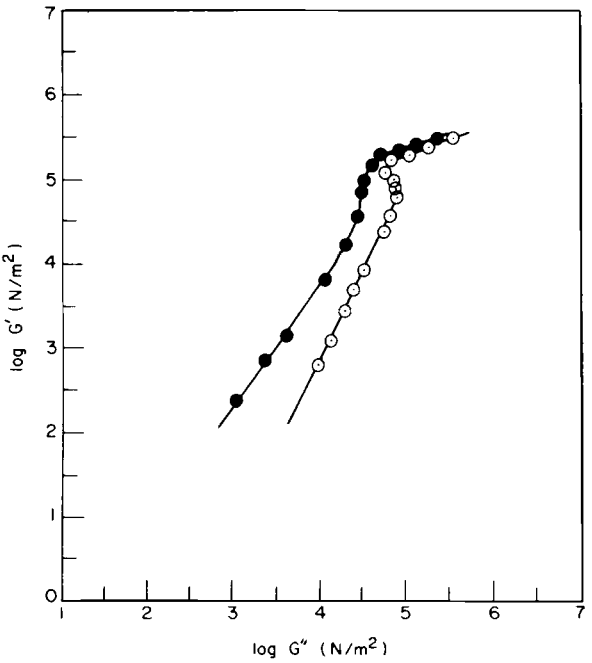

Fig. 10. log G' vs. log G'' for polystyrenes, which are the same materials as in Figure 9: (○) L15; (●) PS7.

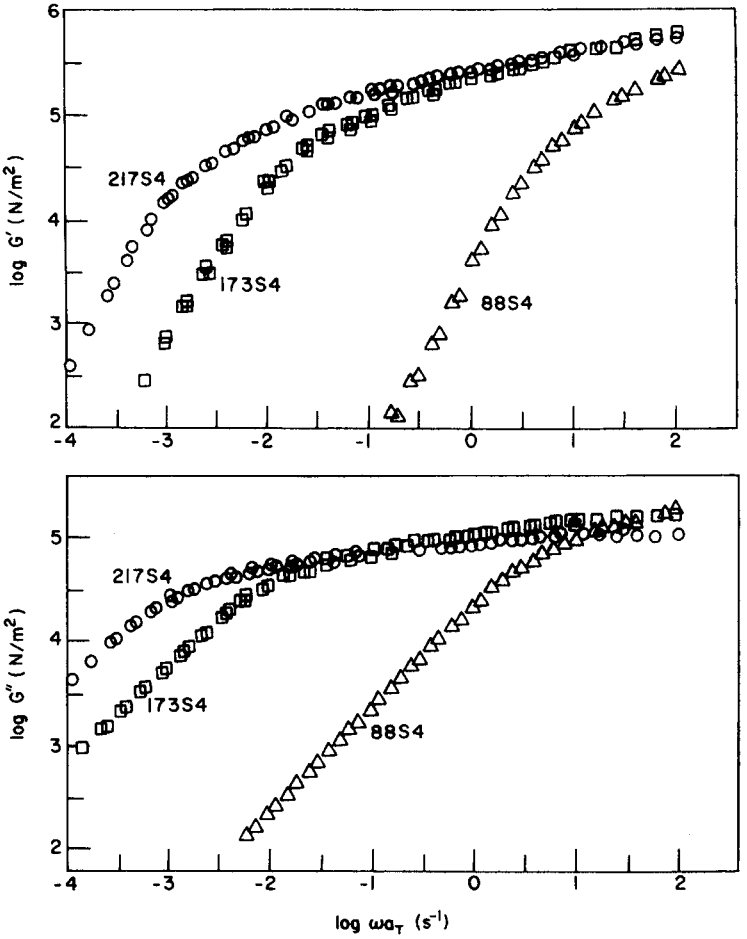

Fig. 11. log G' and log G'' vs. log ωa_T for four-star branched polybutadienes. The reference temperature is 24.5°C.[38]

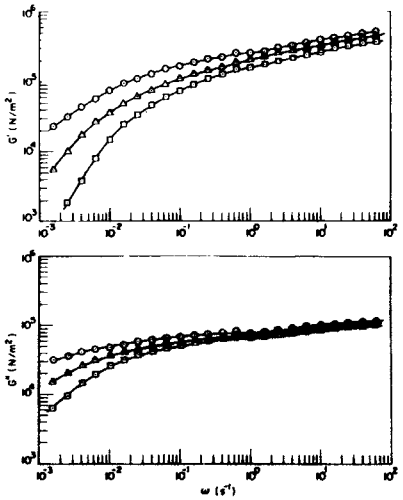

Fig. 12. log G' and log G'' vs. log ω for the four-star branched polybutadiene PB-217S4 at three different temperatures (°C): (○) 24.5; (△) 50; (□) 75.

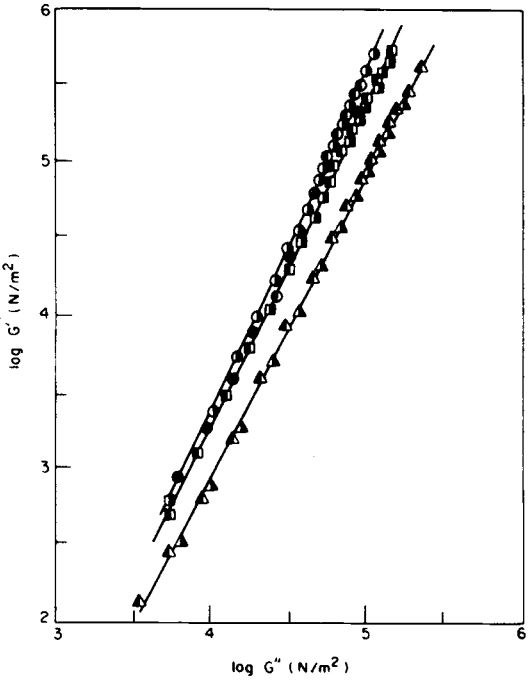

Fig. 13. log G' vs. log G'' for four-star branched polybutadienes, which are the same materials as in Figure 11: (a) 173S4 at 24.5°C (◧) and 50°C (◨); (b) 88S4 at 24.5°C (◭) and 50°C (◮); (c) 217S4 at 24.5°C (◐), 50°C (●), and 75°C (◑).

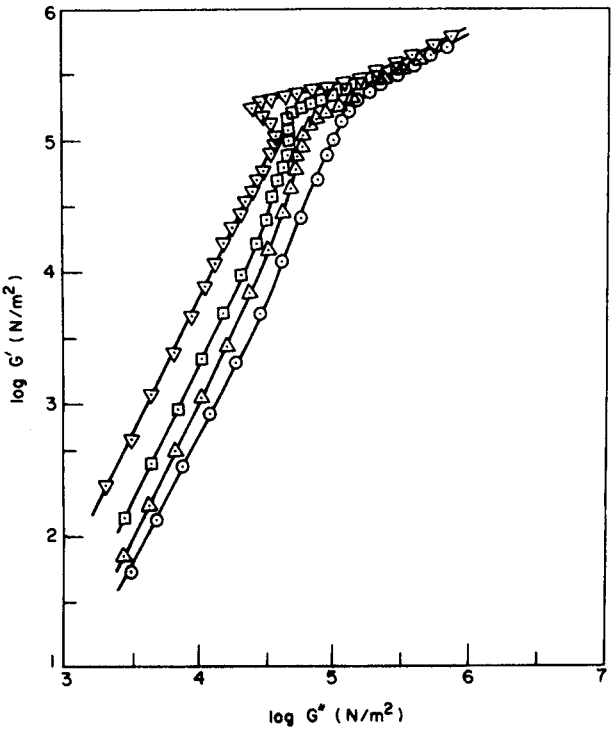

Fig. 14. log G' vs. log G'' for four-arm polystyrenes: (⊙) S121A; (◬) S111A; (⊡) S161A; (▽) S181A. The reference temperature is 170°C.[39]

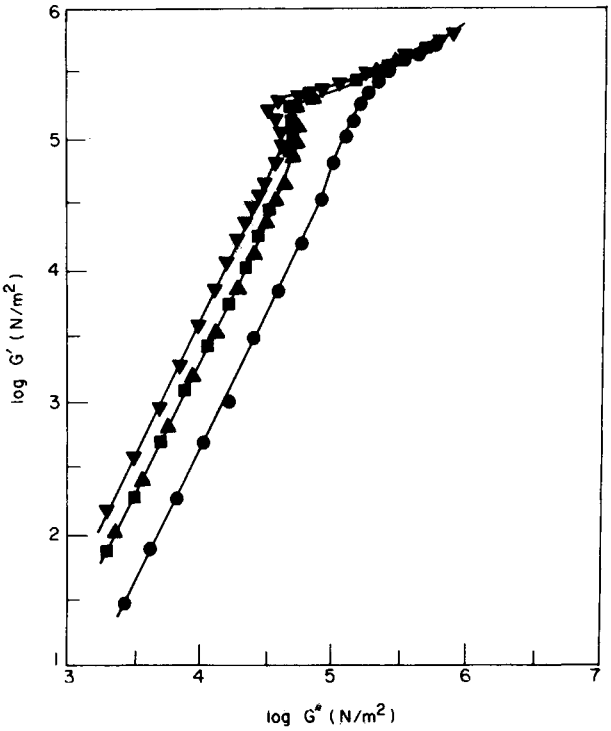

Fig. 15. log G' vs. log G'' for six-arm polystyrenes: (●) HS061A; (▲) HS041A; (■) HS111A; (▼) HS051A. The reference temperature is 170°C.[39]

flow and the loss modulus G'' in oscillatory shear flow may be considered as the amount of energy dissipated. Therefore the N_1/σ_{12} ratio and G'/G'' ratio may be interpreted as the ratio of the energy stored to the energy dissipated.

As pointed out by Han and Lem,[19] in steady shear flow, one may consider the shear rate ($\dot{\gamma}$) to be an input variable imposed on the fluid, whereas both σ_{12} and N_1 are output variables, i.e., responses of the fluid under test. In other words, the values of $\dot{\gamma}$ chosen during experiment have nothing to do with any molecular deformation that occurs, whereas σ_{12} represents the energy dissipated and N_1 represents the energy stored in the fluid. Simi-

TABLE V
Molecular Characteristics Data for Star-Branched Polystyrenes[39]

Sample	$\overline{M}_w \times 10^{-3}$
Four-arm star polystyrene	
S121A	93.5
S111A	154
S161A	351
S181A	1027
Six-arm star polystyrene	
HS061A	110
HS041A	509
HS111A	591
HS051A	1090

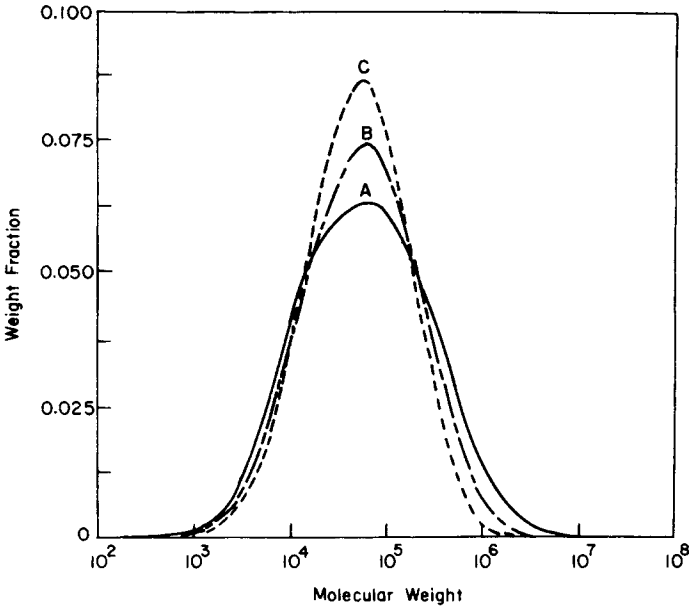

Fig. 16. Molecular weight distribution curves for three different grades of commercial low-density polyethylene.

TABLE VI
Molecular characteristics Data for Low-Density Polyetylenes

Sample	$\overline{M}_w \times 10^{-3}$	$\overline{M}_n \times 10^{-3}$	$\overline{M}_w/\overline{M}_n$	λ_N^a
A	201	21.3	9.43	3.4
B	143	22.5	6.03	2.5
C	110	26.3	4.18	1.6

[a] λ_N represents the long-chain branching frequency, defined as the number-average number of branch point per 1000 carbon atoms.

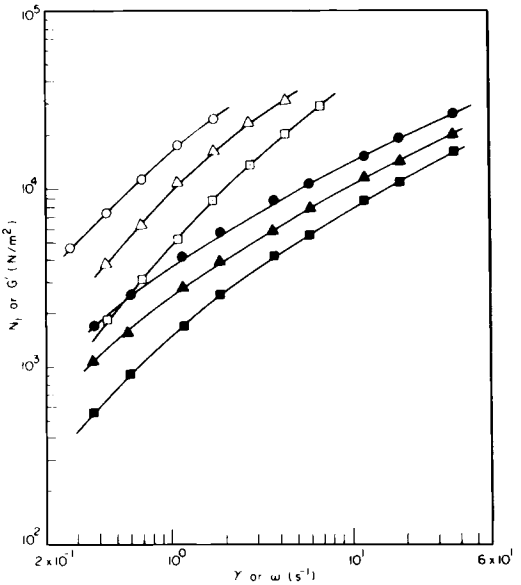

Fig. 17. log N_1 vs. log $\dot{\gamma}$ (open symbols) and log G' vs. log ω (closed symbosl) for a commercial grade low-density polyethylene, LDPE-A: (⊙, ●) 180°C; (△, ▲) 200°C; (⊡, ■) 220°C.

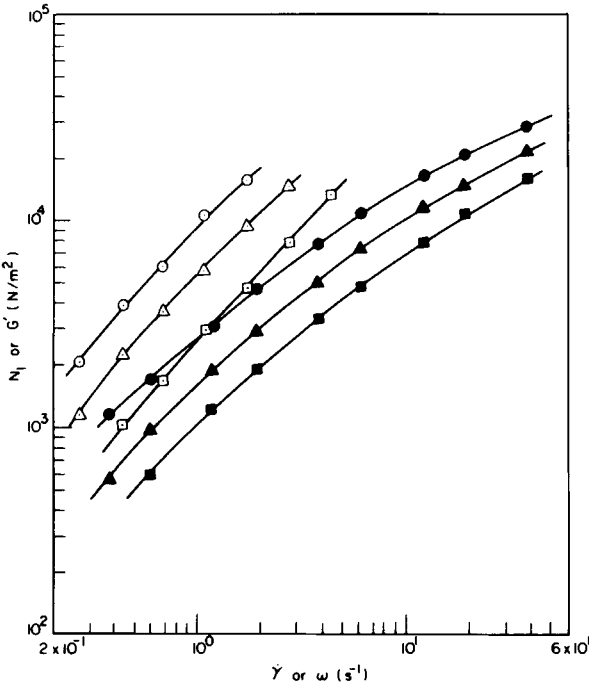

Fig. 18. log N_1 vs. log $\dot{\gamma}$ (open symbols) and log G' vs. log ω (closed symbols) for a commercial grade low-density polyethylene, LDPE-B: (⊙, ●) 180°C; (△, ▲) 200°C; (⊡, ■) 220°C.

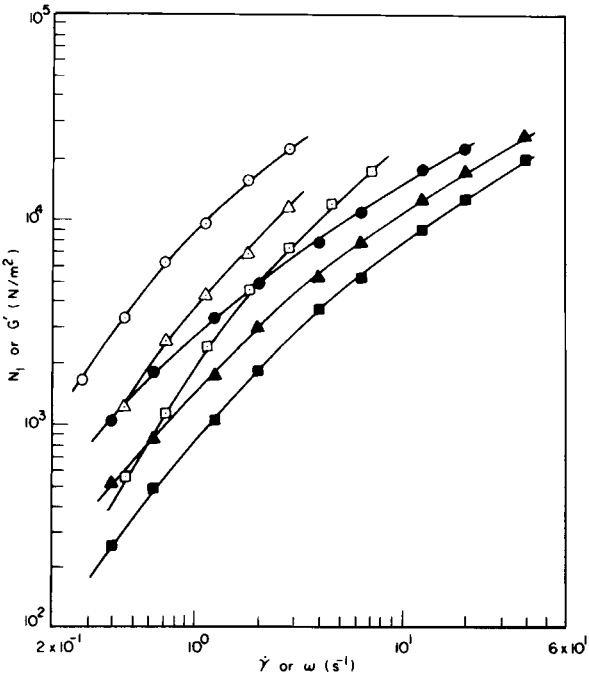

Fig. 19. log N_1 vs. log $\dot{\gamma}$ (open symbols) and log G' vs. log ω (closed symbols) for a commercial grade low-density polyethylene, LDPE-C: (⊙, ●) 180°C; (△, ▲) 200°C; (⊡, ■) 220°C.

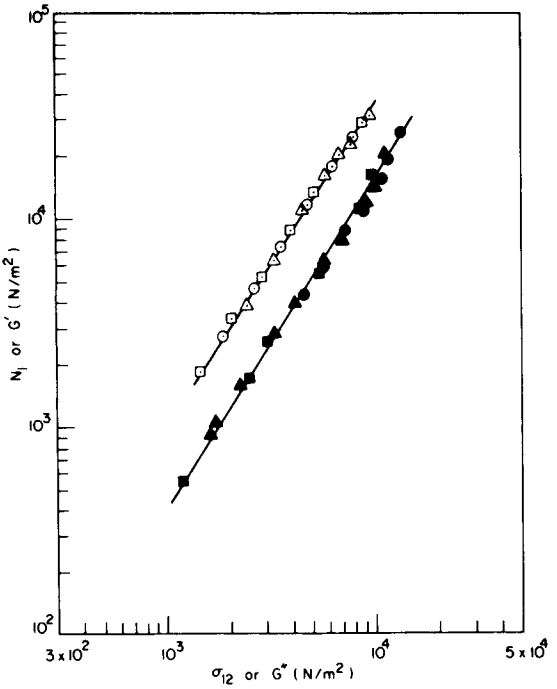

Fig. 20. log N_1 vs. log σ_{12} and log G' vs. log G'' for LDPE-A. Symbols are the same as in Figure 17.

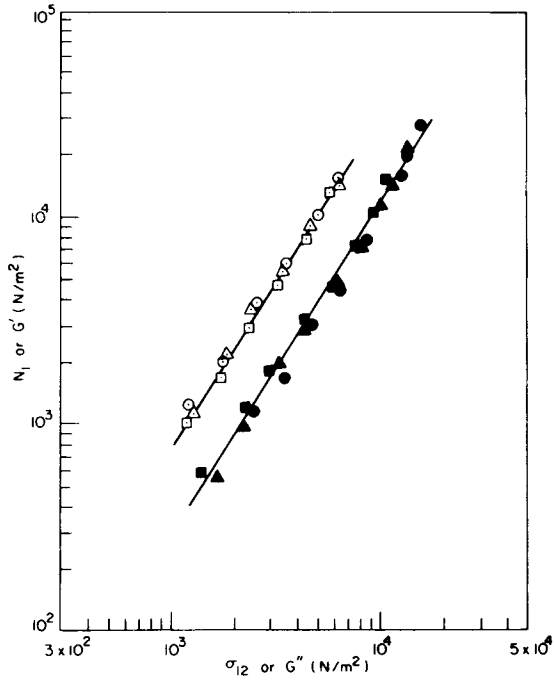

Fig. 21. log N_1 vs. log σ_{12} and log G' vs. log G'' for LDPE-B. Symbols are the same as in Figure 18.

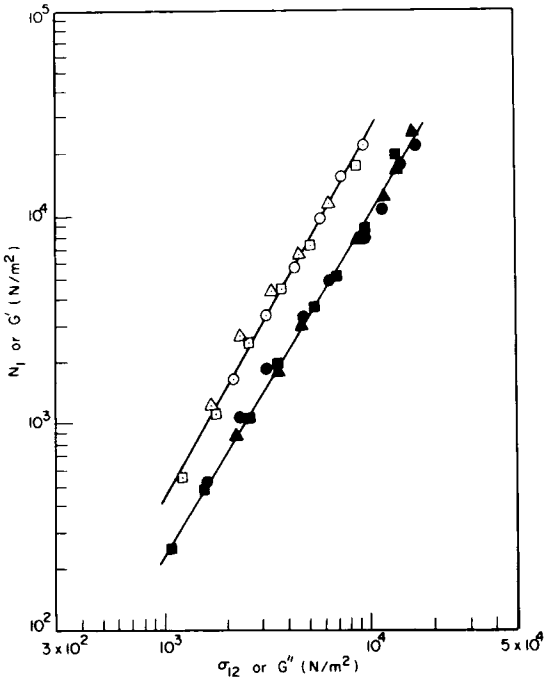

Fig. 22. log N_1 vs. log σ_{12} and log G' vs log G'' for LDPE-C. Symbols are the same as in Figure 19.

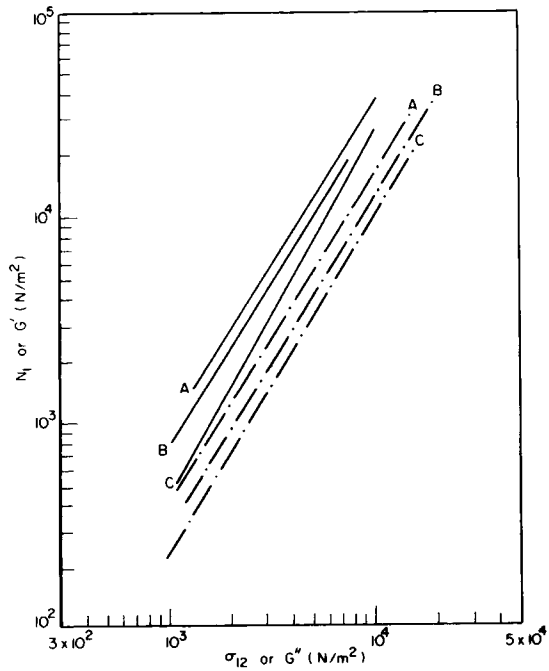

Fig. 23. Comparison of the log N_1–log σ_{12} plots (—) with the log G'—log G'' plots (- • -) for the three different grades of LDPE, described in Figures 20–22.

larly, in oscillatory shear flow, one may consider the oscillatory frequency (ω) to be an input variable and, G' and G'' are output variables (i.e., responses) of the fluid under test. With this interpretation of rheological responses, Han and Lem have suggested that, in order to compare the elastic behavior of one fluid against others, *logarithmic* plots of N_1 vs. σ_{12}, and of G' vs G'', be used.

Following the suggestion of Han and Lem and using a simple dimensional analysis, the output variables G' and G'' in oscillatory shear flow can be represented in terms of the input variable ω by

$$G'_R = G'/G_0 = \mathcal{F}_1(\omega\lambda) \tag{1}$$

and

$$G''_R = G''/G_0 = \mathcal{F}_2(\omega\lambda) \tag{2}$$

in which λ is a relaxation time of the fluid and G_0 is a quantity that has the dimension of stress.

By eliminating $\omega\lambda$ from eqs. (1) and (2), we obtain

$$G'_R = \mathcal{F}_1(\omega\lambda) = \mathcal{F}_1[\mathcal{F}_2^{-1}(G''_R)] = \mathcal{F}(G''_R) \tag{3}$$

Equation (3) implies that the relationship between G'_R and G''_R is independent of the characteristic time of the fluid. Note, however, that plots of G' vs. G'' will depend on the physical parameters of the fluid via G_0. If G_0 is weakly dependent upon temperature and molecular weight, the relationship between G' and G'' will become virtually independent of temperture and molecular weight.

The above statement can be generalized for the system that may be described by more than one characteristic time. In order to demonstrate this, let us assume that the system may be described by N relaxation times. We can, then, represent the output variables G'_R and G''_R in oscillatory shear flow in terms of the input variable ω and N relaxation times by

$$G'_R = F_{1N}(\omega\,;\lambda_1, \lambda_2, \ldots, \lambda_N) \tag{4}$$

and

$$G''_R = F_{2N}(\omega\,;\lambda_1, \lambda_2, \ldots, \lambda_N) \tag{5}$$

By using a dimensional analysis, eqs. (4) and (5) can be rewritten as

$$G'_R = F_1^{(N)}(\omega\lambda_1; \zeta_2, \zeta_3, \ldots, \zeta_N) \tag{6}$$

and

$$G''_R = F_2^{(N)}(\omega\lambda_1; \zeta_2, \zeta_3, \ldots, \zeta_N) \tag{7}$$

where the ζ_p's are defined by

$$\zeta_p = \lambda_p/\lambda_1, \; p = 2, 3, \ldots, N \tag{8}$$

By eliminating $\omega\lambda_1$ from eqs. (6) and (7), we obtain

$$G'_R = F_1^{(N)} [(F_2^{(N)})^{-1}(G''_R; \zeta_2, \ldots, \zeta_N), \zeta_2, \ldots, \zeta_N] \tag{9}$$

It now becomes very obvious from eq. (9) that G'_R–G''_R relationship is independent of fluid properties if ζ_p's are independent of the molecular characteristics of the fluid.

So far we have shown a general relationship between G'_R and G''_R in terms of the relaxation times. In order to interpret the experimental results presented above, however, we must obtain specific functional representations for $\mathcal{F}_1$ and $\mathcal{F}_2$ and, also, for $F_1^{(N)}$ and $F_2^{(N)}$, with ζ_p's and G_0 as parameters. Molecular theory should provide such relationships. Realizing the fact that at present none of the known molecular theories can correctly predict many of the experimental results, we will use the Doi–Edwards theory[46,47] to interpret the experimental results presented above.

In oscillatory shear flow, the Doi–Edwards theory gives the following expressions:

$$G' = \frac{8}{\pi^2} \sum_{p \text{ odd}} \frac{G_0}{p^2} \frac{(\omega\lambda_p)^2}{1 + (\omega\lambda_p)^2} \tag{10}$$

and

$$G'' = \frac{8}{\pi^2} \sum_{p \text{ odd}} \frac{G_0}{p^2} \frac{\omega\lambda_p}{1 + (\omega\lambda_p)^2} \tag{11}$$

in which λ_p is the relaxation time spectrum defined as

$$\lambda_p = \lambda_D/p^2, \; p = 1, 3, 5, \ldots, N \tag{12}$$

where λ_D is the disengagement time defined as

$$\lambda_D = L^2/D\pi^2 \tag{13}$$

In eq. (13), L is an arc length which is proportional to molecular weight, and D is the curvilinear diffusion coefficient which depends on the molecular weight and temperature.

In order to facilitate our analysis here, we will first consider the situation of a single relaxation time, i.e., $p = 1$ in eq. (12). In this situation, eqs. (10) and (11) reduce to

$$G'_R = \frac{(\omega\lambda_D)^2}{1 + (\omega\lambda_D)^2} \tag{14}$$

and

$$G''_R = \frac{\omega\lambda_D}{1 + (\omega\lambda_D)^2} \tag{15}$$

where λ_D is defined by eq. (13). According to the Doi–Edwards theory[47], G_0 that appears in eqs. (10) and (11) is proportional to the absolute temperature T,

$$G_0 = c_1 kT/M_e \tag{16}$$

where c_1 is a constant, k is the Boltzmann constant, and M_e is the average molecular weight between entanglement points. Note that G_0 is the plateau modulus that depends on temperature but not on molecular weight, and that the specific expression for G_0 would vary with the rheological model chosen.

By eliminating $\omega\lambda_D$ from eqs. (14) and (15), we obtain

$$(G'_R)^2 + (G''_R)^2 = G'_R \tag{17}$$

or

$$(G'_R - 0.5)^2 + (G''_R)^2 = (0.5)^2 \tag{18}$$

Equation (17) gives the following relationships between G'_R and G''_R:

$$\text{(i)}\ G'_R = (1 - \sqrt{1 - 4(G''_R)^2})/2 \tag{19}$$

and

$$\text{(ii)}\ G'_R = (1 + \sqrt{1 - 4(G''_R)^2})/2 \tag{20}$$

Note that, in order for eqs. (19) and (20) to have a physical significance, G''_R must be smaller than 0.5. It can easily be shown that this restriction is statisfied in the physical systems considered in Figures 1–22.

Figure 24 gives a schematic describing the relationship between G'_R and G''_R on the logarithmic scale. The following limiting cases of eq. (17) are of practical interest here.

(i) In Region 1 (i.e., for $\omega\lambda_D << 1$), from eqs. (14) and (15) we have

$$G'_R = (G''_R)^2 \tag{21}$$

(ii) In Region 3 (i.e., for $\omega\lambda_D >> 1$), from eqs. (14) and (15) we have

$$G'_R = 1 - (G''_R)^2 \tag{22}$$

Note that Region 3 may not be reacheable experimentally.

(iii) In Region 2, we observe that the curve changes its direction at $G'_R = G''_R = 0.5$. Indeed such behavior has been observed experimentally, as

displayed in Figure 2. In order to facilitate our discussion here, let us define the quantities ξ' and ξ'' by

$$\xi' = G'_R - G_* \tag{23}$$

and

$$\xi'' = G_* - G''_R \tag{24}$$

Substituting eqs. (23) and (24) into eq. (17), with the aid of the relationship, $G'_R = G''_R = G_* = 0.5$ that follows from eqs. (19) and (20), we have

$$(\xi')^2 = \xi'' - (\xi'')^2 \tag{25}$$

For small values of ξ'' (i.e., near the turning point of the curve given in Figure 24), eq. (25) reduces to

$$(\xi')^2 = \xi'' \tag{26}$$

or

$$(G'_R - 0.5)^2 = (0.5 - G''_R) \tag{27}$$

Rewriting eq. (21) in terms of G' and G'', we obtain

$$G' = (G'')^2/G_0 \tag{28}$$

Taking logarithms of both sides of eq. (28), we obtain

$$\log G' = 2 \log G'' - \log G_0 \tag{29}$$

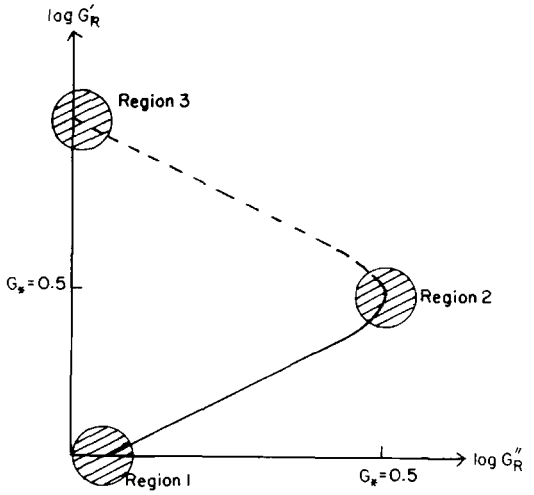

Fig. 24. Schematic describing the relationship between G'_R and G''_R, given by eq. (17), on logarithmic coordinates.

It is clear from eq. (29) that log G' is proportional to log G'' with a slope of 2. It is of special interest to note that the slope of the log G'–log G'' plot is independent of temperature. With G_0 defined by eq. (16), we observe in eq. (29) that an increase of temperature from T_1 to T_2 will shift the value of log G' by the amount log (T_1/T_2). More specifically, an increase of temperature from 25.5 to 75°C for the linear PB-347L will shift the value of log G' by the amount 0.068 N/m^2 (see Fig. 4), and an increase of temperature from 180 to 220°C for the LDPE-A will shift the value of log G' by the amount 0.0539 N/m^2 (see Fig. 20). Such an insignificant amount of shift in log G' is not noticeable in the log G'–log G'' plots. We now understand the reason why log G'–log G'' plots show correlations that are only slightly sensitive to (or virtually independent of) temperature, as demonstrated in Figures 4, 13, 20, 21, and 22.

Let us now consider the effect of molecular weight on the log G'–log G'' plot. According to eq. (16), G_0 does not depend on molecular weight and therefore the log G'–log G'' plot [i.e., the use of eq. (3)] does not show molecular weight dependence. It can be concluded therefore that for high molecular weight polymers with narrow molecular weight distributions, log G'–log G'' plots do *not* depend on their molecular weights. This now explains why only a very weak dependence of molecular weight is seen in the log G'–log G'' plots displayed in Figures 2, 6, and 8.

It should be pointed out that eqs. (3) and (17) are derived on the basis of the assumption that relaxation times can be represented by the reptation motion only. However, on the high frequency side (i.e., in the transition region), the log G'–log G'' plot may depend on temperature and molecular weight, as may be seen, for instance, in Figures 2 and 4. Therefore, in the transition region, in addition to the reptation motion, the Rouse motion of polymer chains between entanglement points may contribute to relaxation times. Note that these two relaxation times have a different molecular weight dependence, and ζ_p defined in eq. (8) is not constant. In such instances, the output variables (i.e., responses) G'_R and G''_R in oscillatory shear flow can be represented in terms of the input variable ω and relaxation times by

$$G'_R = F_3(\omega\,;\lambda_D, \lambda_{eq}) = \mathcal{F}_3(\omega\lambda_D, \zeta_2) \tag{30}$$

and

$$G''_R = F_4(\omega\,;\lambda_D, \lambda_{eq}) = \mathcal{F}_4(\omega\lambda_D, \zeta_2) \tag{31}$$

in which λ_{eq} denotes the equilibrium time associated with the Rouse motion of polymer chains, and $\zeta_2 = \lambda_{eq}/\lambda_D$.

By eliminating $\omega\lambda_D$ from eqs. (30) and (31), we obtain

$$G'_R = \mathcal{F}_5(G''_R, \zeta_2) \tag{32}$$

Since ζ_2 is weakly dependent upon temperature, but strongly dependent upon molecular weight, the log G'–log G'' plot may show strong dependence on molecular weight in the transition region.

DISCUSSION

The log N_1–log σ_{12} Plot

We will now explain why log N_1 – log σ_{12} plots also show slight sensitivity to a variation in temperature (see Fig. 20–22), using the same argument as that used above in discussing oscillatory shear flow. In steady shear flow, the output variables σ_{12} and N_1 can be related to the input variable $\dot{\gamma}$ by

$$S_1 = \sigma_{12}/\sigma_0 = U_1(\lambda\dot{\gamma}) \tag{33}$$

and

$$S_2 = N_1/\sigma_0 = U_2(\lambda\dot{\gamma}) \tag{34}$$

in which λ is a characteristic time of the fluid under test and σ_0 is a quantity that has the dimension of stress. Note that the functional form of U_1 in eq. (33) and U_2 in eq. (34) depends on the choice of rheological model. There are a number of rheological models suggested in the literature. In order to demonstrate our basic idea, we will choose a relatively simple one, known as the Zaremba–DeWitt model[48,49]

$$\tau + \lambda(\mathscr{D}\tau/\mathscr{D}t) = 2\,\eta_0\mathbf{d} \tag{35}$$

where τ and $\mathbf{d}$ are stress and rate-of-deformation tensors, respectively, $\mathscr{D}/\mathscr{D}t$ is the Jaumann derivative, η_0 is the zero-shear viscosity, and λ is the terminal relaxation time (i.e., the longest relaxation time observed in mechanical measurements). It can be shown[50] that, in steady shear flow, eq. (35) gives:

$$\sigma_{12} = \frac{\sigma_0\lambda\dot{\gamma}}{1 + (\lambda\dot{\gamma})^2} \tag{36}$$

and

$$N_1 = \frac{2\sigma_0(\lambda\dot{\gamma})^2}{1 + (\lambda\dot{\gamma})^2} \tag{37}$$

in which σ_0 is defined by

$$\sigma_0 = \eta_0/\lambda \tag{38}$$

The use of eqs. (36) and (37) in eqs. (33) and (34) and elimination of $\lambda\dot{\gamma}$ from the resulting expressions yields

$$(S_1)^2 + (0.5S_2)^2 = 0.5S_2 \tag{39}$$

It is of great interest to note that the form of eq. (39) is identical to that

of eq. (17), with S_1 being equivalent to G''_R *and* $0.5S_2$ being equivalent to G'_R. Equation (39) gives the following relationships between S_1 and S_2:

$$S_2 = 1 - \sqrt{1 - 4(S_1)^2} \tag{40}$$

and

$$S_2 = 1 + \sqrt{1 - 4(S_1)^2} \tag{41}$$

for which the restriction $S_1 \leq 0.5$ must be satisfied.

It can be shown easily that, for small values of S_1 and S_2, eq. (40) reduces to

$$0.5S_2 = (S_1)^2 \tag{42}$$

or

$$N_1 = 2(\sigma_{12})^2/\sigma_0 \tag{43}$$

Note that the form of eq. (43) is identical to that of eq. (28) and, that the $\log N_1 - \log \sigma_{12}$ plot of eq. (43) gives a slope of 2.

At this juncture, it is worth elaborating on the physical significance of σ_0 defined in eq. (38), in conjunction with the use of eq. (43). According to de Gennes,[51] σ_0 is the modulus of a polymeric liquid and may be expressed as

$$\sigma_0 = c_2 T/M_e \tag{44}$$

where c_2 is a constant, T, is the temperature, and M_e represents the average interval between entanglement points. Therefore, the $\log N_1 - \log \sigma_{12}$ plot of eq. (43), with the aid of eq. (44), will give a very weak dependence on temperature, which indeed has been demonstrated in Figures 20–22. According to de Gennes,[51] M_e appearing in eq. (44) includes the effects of entanglements between the molecules and therefore the use of eq. (44) in eq. (43) reveals that $\log N_1 - \log \sigma_{12}$ plots will be independent of molecular weight. These conclusions are exactly the same as those made above in discussing the effect of temperature and molecular weight on $\log G' - \log G''$ plots for high molecular weight polymers.

It is of interest to observe that the data displayed in Figures 20–22 may be represented by the following empirical expression:

$$N_1 = a(\sigma_{12})^b \tag{45}$$

with the value of b (i.e., the slope of the $\log N_1 - \log \sigma_{12}$ plots) ranging from 1.55 to 1.80, which is independent of temperature within the range of temperature tested (also, of course, within measurement errors). Note, however, that the values of a and b appearing in eq. (45) seem to depend on the molecular weight, molecular weight distribution, and the degree of side-chain branching. As a matter of fact, Han and co-workers[13,15,16,20–23] and

White and co-workers[25,26] have reported experimental observations that may also be represented by eq. (45).

The Cole–Cole Plot

It seems appropriate to discuss, at this juncture, the differences between the log G'–log G'' plot and the Cole–Cole plot. In 1941, Cole and Cole[41] first used plots of the imaginary part ϵ'' of the complex dielectric constant against the real part ϵ', for a number of polar materials at various temperatures. It should be pointed out that the Cole–Cole plot uses ϵ'' as ordinate and ϵ' as abscissa in the ordinary coordinate system. They reported that ϵ''–ϵ' plots fell on a circular arc and that a different arc was found for each temperature, with the shape of the circular arc varying with temperature.

It should be noted that, in general, G_0 depends on temperature and molecular weight and the nature of the dependency is specified by the molecular model chosen. For example, the modified Rouse model, which is applicable to undiluted polymers having narrow molecular weight distributions and molecular weights below about 20,000, gives[3]

$$G_0 = \rho RT/M \tag{46}$$

in which ρ is the density, R is the universal gas constant, T is the absolute temperature, and M is the molecular weight. In contrast, G_0 depends only on temperature in the case of the Doi–Edwards theory [see eq. (16)].

For illustration purposes, let us consider the modified Rouse theory. It is seen that eq. (18) represents a circle with its center at $G'_R = 0.5$ and $G''_R = 0$, and having a radius of 0.5. Let us examine how the temperaure and molecular weight affect the size of the circular arc. For convenience, let us define the folowing quantities:

$$\tilde{G}'_R(T) = G'(T)/G_0(T_0) \tag{47}$$

and

$$\tilde{G}''_R(T) = G''(T)/G_0(T_0) \tag{48}$$

where T_0 is a reference temperature. Note that $G_0(T_0)$ is defined by eq. (46) with $T = T_0$. With the aid of eq. (1), we have

$$G'_R(T) = \frac{G'(T)}{G_0(T)} = \frac{G'(T)}{G_0(T_0)}\frac{G_0(T_0)}{G_0(T)} = \tilde{G}'_R(T)\frac{T_0}{T} \tag{49}$$

and in a similar fashion, with the aid of eq. (2), we have

$$G''_R(T) = \tilde{G}''_R(T)\frac{T_0}{T} \tag{50}$$

Substitution of eqs. (49) and (50) into eq. (18) gives

$$\left[\tilde{G}'_R - \frac{1}{2}\frac{T}{T_0}\right]^2 + (\tilde{G}''_R)^2 = \left[\frac{1}{2}\frac{T}{T_0}\right]^2 \tag{51}$$

Note from eqs. (47) and (48) that the dependence of $\tilde{G}'_R$ and $\tilde{G}''_R$ on temperature is just the same as the dependence of G' and G'' on temperature. However, the dependence of G'_R and G''_R on temperture is *not* the same as the dependence of G' and G'' on temperature.

Equation (51) desceibes the explicit dependence of $\tilde{G}'_R$ and $\tilde{G}''_R$ (and, thus, of G' and G'') on temperature. If for example, the temperature is increased from 180 to 220°C, with a reference temperature at $T_0 = 180$°C, eq. (51) becomes

$$(\tilde{G}'_R - 0.544)^2 + (\tilde{G}''_R)^2 = (0.554)^2 \tag{52}$$

The Cole–Cole plot of eq. (52) is given in Figure 25, showing a clear temperature dependence with the diameter of the circle increased by 8.8%. Figures 26–28 give plots of G'' vs. G' (i.e., Cole–Cole plots) for the three LDPEs considered in Figures 20–22. It is seen that such plots show a strong temperature dependence.

On the other hand, when eq. (52) is plotted on logarithmic graph paper, temperature effect is very much suppressed as shown in Figure 29. Within experimental error, such a small difference may not be distinguishable in log $\tilde{G}'$ – log $\tilde{G}''$ plots. Indeed, this has been the case, as demonstrated experimentally in Figures 20–22.

Again, using the modified Rouse theory for illustration purposes, let us examine the effect of molecular weight on G' and G''. For convenience, let us define the following quantities:

$$\tilde{\tilde{G}}'_R(M) = G'(M)/G_0(M_0) \tag{53}$$

and

$$\tilde{G}''_R(M) = G''(M)/G_0(M_0) \tag{54}$$

in which M_0 is a reference molecular weight. Note that $G_0(M_0)$ is defined by eq. (46) with $M = M_0$. With the aid of eq. (1), we have

$$G'_R(M) = \frac{G'(M)}{G_0(M_0)}\frac{G_0(M_0)}{G_0(M)} = \tilde{\tilde{G}}'_R(M)\frac{M}{M_0} \tag{55}$$

and in a similar fashion, with the aid of eq. (2), we have

$$G''_R(M) = \tilde{\tilde{G}}''_R(M)\frac{M}{M_0} \tag{56}$$

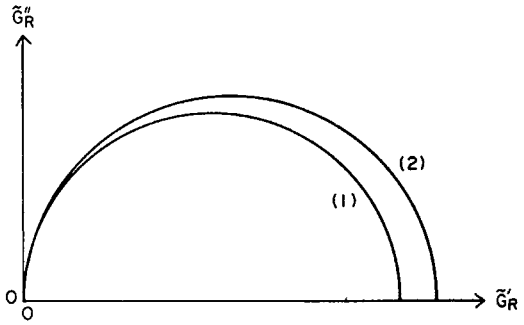

Fig. 25. Cole–Cole plot of eq. (51): (1) $T/T_0=1$; (2) $T/T_0=1.088$. The reference temperature T_0 is 180°C.

Substitution of eqs. (55) and (56) into eq. (18) gives

$$\left[\tilde{\tilde{G}}'_R - \frac{1}{2}\frac{M_0}{M}\right]^2 + (\tilde{\tilde{G}}''_R)^2 = \left[\frac{1}{2}\frac{M_0}{M}\right]^2 \tag{57}$$

Equation (57) describes the explicit dependence of $\tilde{\tilde{G}}'_R$ and $\tilde{\tilde{G}}''_R$ (and thus of G' and G'') on molecular weight.

With the choice of $M_0=5000$ as a reference molecular weight for illustration purposes, the Cole–Cole plot of eq. (57) for $M=500$ is given in Figure 30, and the corresponding log $\tilde{\tilde{G}}'_R$–log $\tilde{\tilde{G}}''_R$ plot is given in Figure 31. It is seen that molecular weight dependence is seen in the log $\tilde{\tilde{G}}'_R$–log $\tilde{\tilde{G}}''_R$ plot

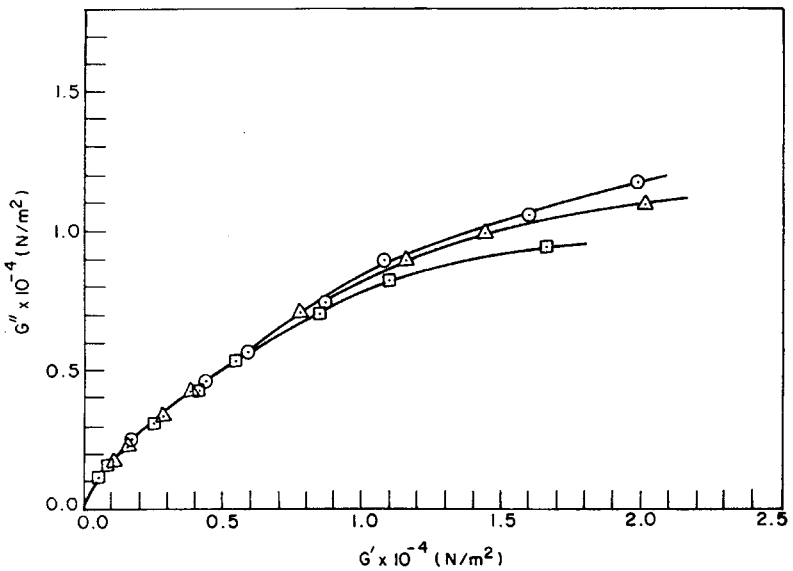

Fig. 26. Cole–Cole plot for LDPE-A at three different temperatures (°C): (⊙) 180; (△) 200; (□) 220.

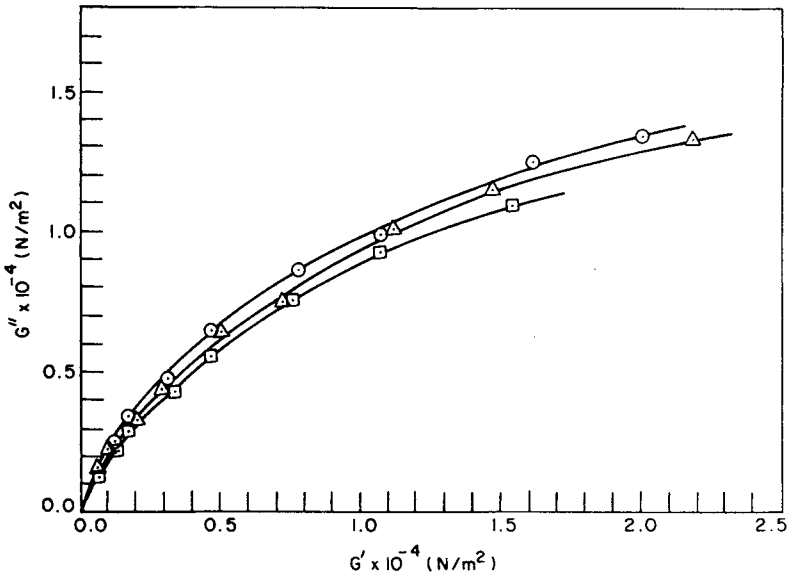

Fig. 27. Cole–Cole plot for LDPE-B at three different temperatures. The symbols are the same as in Figure 26.

as strongly as in the Cole–Cole plot. Note that this strong molecular weight dependence in the Cole–Cole plot is due to the particular model (i.e., the modified Rouse model) chosen for illustration purposes. If one adopts the Doi–Edwards theory, there would be no molecular weight dependence in the log $\tilde{\tilde{G}}'_R$–log $\tilde{\tilde{G}}''_R$ plot since G_0 is independent of molecular weight.

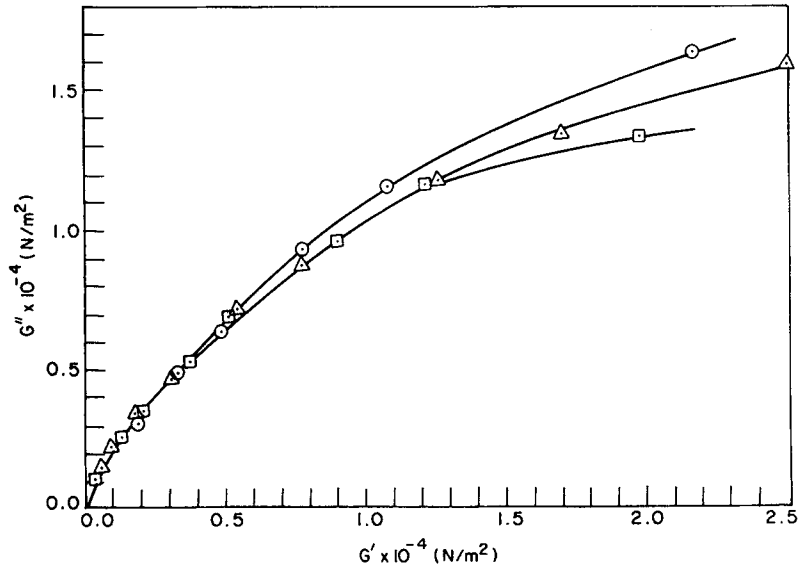

Fig. 28. Cole–Cole plot for LDPE-C at three different temperatures. The symbols are the same as in Figure 26.

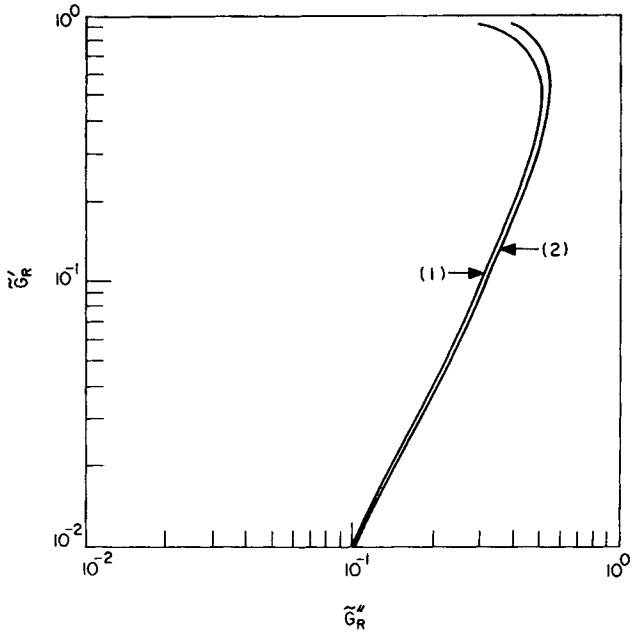

Fig. 29. Logarithmic plot of eq. (51): (1) $T/T_0=1$; (2) $T/T_0=1.088$. The reference temperature T_0 is 180°C.

CONCLUSIONS

Based on the experimental data presented and the theoretical analysis carried out in this paper, we can conclude that the log G'–log G'' and log N_1–log σ_{12} plots are very useful for investigating the elastic responses of viscoelastic polymeric liquids, in particular bulk homopolymers. It is shown that such plots give rise to correlations which are weakly sensitive to a variation in temperature.

Using the Doi–Edwards theory as an example, we have shown that the log G'–log G'' plot shows little sensitivity to a variation in temperature. We have also shown that the log G'–log G'' plot becomes independent of

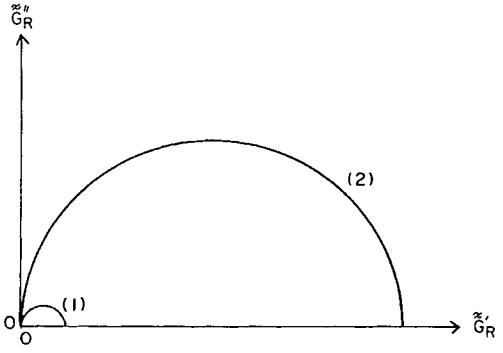

Fig. 30. Cole–Cole plot of eq. (57): (1) $M_0/M=1$; (2) $M_0/M=10$. The reference molecular weight M_0 is 5000.

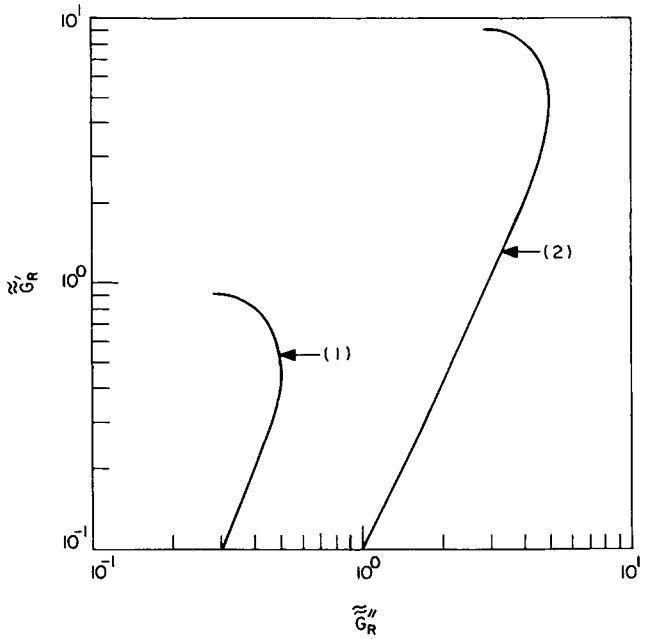

Fig. 31. Logarithmic plot of eq. (57): (1) $M_0/M=1$; (2) $M_0/M=10$. The reference molecular weight M_0 is 5000.

molecular weight for high molecular weight polymers whose molecular weights are greater than the average molecular spacing between entanglements M_e, i.e., when entanglement effects are important. We have shown further, with the aid of molecular theories, that the log G'–log G'' plot shows dependence on molecular weight distribution. Using the Zaremba–DeWitt model as an example, we have explained why the log N_1–log σ_{12} plot gives rise to a correlation which becomes weakly sensitive to a variation in temperature.

We wish to acknowledge that Dr. W. W. Graessley at Exxon Research and Engineering Co. supplied us with the numerical data used in Figures 3, 4, 12, and 13, and Dr. J. Roovers of the National Research Council of Canada supplied us with the numerical data used in Figures 14 and 15.

References

1. K. Walters, *Rheometry*, Chapman and Hall, London, 1975.
2. K. Walters, Ed., *Rheometry: Industrial Applications*, Wiley, New York, 1980.
3. J. D. Ferry, *Viscoelastic Properties of Polymers*, 3rd ed., Wiley, New York, 1980, Chap. 5.
4. J. W. C. Adamse, H. Janeschitz-Kriegl, J. L. den Otter, and J. L. S. Wales, *J. Polym. Sci., Part A-2*, **6**, 871 (1968).
5. C. D. Denson, W. M. Prest, and M. O'Reilly, *AIChE J.*, **15**, 809 (1969).
6. C. D. Han, K. U. Kim, N. Siskovic, and C. R. Huang, *Rheol. Acta*, **14**, 533 (1975).
7. B. D. Coleman and H. Markovitz, *J. Appl. Phys.*, **35**, 1 (1964).
8. C. D. Han and T. C. Yu, *Rheol. Acta*, **10**, 398 (1971).
9. C. D. Han, K. U. Kim, J. Parker, N. Siskovic, and C. R. Huang, *Appl. Polym. Symp.*, **21**, 191 (1973).
10. C. D. Han, *J. Appl. Polym. Sci.*, **17**, 1289 (1973); **19**, 1875 (1975).
11. C. D. Han and Y. W. Kim, *Trans. Soc. Rheol.*, **19**, 245 (1975).
12. C. D. Han, Y. W. Kim and S. J. Chen, *J. Appl. Polym. Sci.*, **19**, 2831 (1975).

13. C. D. Han, *Rheology in Polymer Processing*, Academic, New York, 1976, Chaps. 5, 7, 10.
14. C. D. Han and R. Shetty, *Polym. Eng. Sci.*, **18**, 180 (1978).
15. C. D. Han and C. A. Villamizar, *J. Appl. Polym. Sci.*, **22**, 1677 (1978).
16. C. D. Han and D. A. Rao, *J. Appl. Polym. Sci.*, **24**, 225 (1979).
17. C. D. Han and D. A. Rao, *Polym. Eng. Sci.*, **20**, 128 (1980).
18. C. D. Han, *Multiphase Flow in Polymer Processing*, Academic, New York, 1981.
19. C. D. Han and K. W. Lem, *Polym. Eng. Rev.*, **2**, 135 (1983).
20. C. D. Han, Y. J. Kim, and H. K. Chuang, *Polym. Eng. Rev.*, **3**, 1 (1983).
21. C. D. Han, Y. J. Kim, H. K. Chuang, and T. H. Kwack, *J. Appl. Polym. Sci.*, **28**, 3435 (1983).
22. H. K. Chuang and C. D. Han, *J. Appl. Polym. Sci.*, **29**, 2205 (1984).
23. H. K. Chuang and C. D. Han, in *Polymer Blends and Composites in Multiphase Systems*, C. D. Han, Ed., Adv. Chem. Ser. No. 206, Am. Chem. Soc., Washington, D.C., 1984, p. 171.
24. C. D. Han and H. K. Chuang, *J. Appl. Polym. Sci.*, **30**, 2431 (1985).
25. K. Oda, J. L. White, and E. S. Clark, *Polym. Eng. Sci.*, **18**, 25 (1978).
26. W. Minoshima, J. L. White, and J. E. Spruiell, *Polym. Eng. Sci.*, **20**, 1166 (1980).
27. H. Yamane and J. L. White, *Polym. Eng. Rev.*, **2**, 167 (1983).
28. B. Liang, J. L. White, J. E. Spruiell, and B. C. Goswami, *J. Appl. Polym. Sci.*, **28**, 2011 (1983).
29. Y. Shimomura, J. E. Spruiell, and J. L. White, *Polym. Eng. Rev.*, **2**, 417 (1983).
30. K. Min, J. L. White, and J. E. Fellers, *J. Appl. Polym. Sci.*, **29**, 2117 (1984).
31. S. Onogi, T. Masuda, and T. Ibaragi, *Koll. Z. Z. Polym.*, **222**, 110 (1968).
32. S. Onogi, T. Masuda, and K. Kitagawa, *Macromolecules*, **3**, 109 (1970).
33. T. Masuda, K. Kitagawa, and S. Onogi, *Macromolecules*, **3**, 116 (1970).
34. T. Masuda, K. Kitagawa, and S. Onogi, *Polym. J.*, **1**, 418 (1970).
35. S. Onogi, T. Masuda, and N. Toda, *Polym. J.*, **1**, 542 (1970).
36. T. Masuda, Y. Ohta, and S. Onogi, *Macromolecules*, **4**, 763 (1971).
37. S. Futamura and E. A. Meinecke, *Polym. Eng. Sci.*, **17**, 563 (1977).
38. W. E. Rochefort, G. G. Smith, H. Rachapudy, V. R. Raju, and W. W. Graessley, *J. Polym. Sci., Polym. Phys. Ed.*, **17**, 1197 (1979).
39. W. W. Graessley and J. Roovers, *Macromolecules*, **12**, 959 (1979).
40. V. R. Raju, E. V. Menzes, G. Marin, W. W. Graessley, and L. T. Fetters, *Macromolecules*, **14**, 1668 (1981).
41. K. S. Cole and R. H. Cole, *J. Chem. Phys.*, **9**, 341 (1941).
42. A. W. Nolle, *J. Polym. Sci.*, **5**, 1 (1950).
43. S. Takahashi, *J. Colloid Sci.*, **9**, 313 (1954).
44. S. V. Kanakkanatt, *J. Cell. Plast.*, **9**, 54 (1973).
45. E. R. Harrell and N. Nakajima, *J. Appl. Polym. Sci.*, **29**, 995 (1984).
46. M. Doi and S. F. Edwards, *J. Chem. Soc. Faraday Trans. II*, **74**, 1789, 1802, 1818 (1978).
47. M. Doi and S. F. Edwards, *J. Chem. Soc. Faraday Trans. II*, **75**, 38 (1979).
48. S. Zaremba, *Bull. Inst. Acad. Sci. Cracovie*, 594 (1903).
49. T. W. DeWitt, *J. Appl. Phys.*, **26**, 889 (1955).
50. C. D. Han, *Rheology in Polymer Processing*, Academic, New York, 1976, p. 38.
51. P. de Gennes, *Scaling Concepts in Polymer Physics*, Cornell Univ. Press, Ithaca, NY, 1979, p. 221.

Received April 4, 1985
Accepted June 28, 1985